

SFC-GAN: A Generative Adversarial Network for Brain Functional and Structural Connectome Translation

Yee-Fan Tan
School of IT

Monash University Malaysia
Subang Jaya, Malaysia
tan.yeefan@monash.edu

Jun Lin Liow
School of IT

Monash University Malaysia
Subang Jaya, Malaysia
junlin.liow7@gmail.com

Pei-Sze Tan
School of IT

Monash University Malaysia
Subang Jaya, Malaysia
tan.peisze@monash.edu

Fuad Noman
School of IT

Monash University Malaysia
Subang Jaya, Malaysia
fuad.noman@monash.edu

Raphaël C.-W. Phan
School of IT

Monash University Malaysia
Subang Jaya, Malaysia
raphael.phan@monash.edu

Hernando Ombao
Statistics Program

King Abdullah University of Science and Technology
Thuwal, Saudi Arabia
hernando.ombao@kaust.edu.sa

Chee-Ming Ting
School of IT

Monash University Malaysia
Subang Jaya, Malaysia
ting.cheeming@monash.edu

Abstract—Modern brain imaging technologies have enabled the detailed reconstruction of human brain connectomes, capturing structural connectivity (SC) from diffusion MRI and functional connectivity (FC) from functional MRI. Understanding the intricate relationships between SC and FC is vital for gaining deeper insights into the brain’s functional and organizational mechanisms. However, obtaining both SC and FC modalities simultaneously remains challenging, hindering comprehensive analyses. Existing deep generative models typically focus on synthesizing a single modality or unidirectional translation between FC and SC, thereby missing the potential benefits of bi-directional translation, especially in scenarios where only one connectome is available. Therefore, we propose Structural-Functional Connectivity GAN (SFC-GAN), a novel framework for bidirectional translation between SC and FC. This approach leverages the CycleGAN architecture, incorporating convolutional layers to effectively capture the spatial structures of brain connectomes. To preserve the topological integrity of these connectomes, we employ a structure-preserving loss that guides the model in capturing both global and local connectome patterns while maintaining symmetry. Our framework demonstrates superior performance in translating between SC and FC, outperforming baseline models in similarity and graph property evaluations compared to ground truth data, each translated modality can be effectively utilized for downstream classification.

Index Terms—Generative adversarial networks, functional connectivity, structural connectivity, fMRI, dMRI

I. INTRODUCTION

Advancements in brain imaging and tracking technologies have enabled detailed reconstruction of human brain connectomes, where nodes represent distinct brain regions and network edges capture either structural connectivity (SC) or functional connectivity (FC). SC corresponds to white matter pathways inferred from diffusion magnetic resonance imaging (dMRI), while FC reflects statistical relationships derived from functional signals like functional magnetic resonance

imaging (fMRI) [1]. Understanding the intricate relationship between SC and FC is essential for gaining deeper insights into the brain’s functional and organizational mechanisms and how these might be disrupted in neurological disorders [2], [3]. Prior studies have shown a strong correlation between SC and FC [4], and both modalities provide complementary information, which can significantly improve the accuracy of brain disorder diagnosis [5]–[8]. However, obtaining both SC and FC data simultaneously is often challenging.

Deep learning models have shown significant promise in synthesizing high quality brain network data, such as generating brain FC [7], [9]–[13] or SC [9], [11], [14], for downstream classification tasks. Nonetheless, these approaches typically focus on a single modality of connectomes, failing to address the challenges posed by the absence of both SC and FC.

To tackle the above issue, recent works have leveraged graph-based neural networks in relating human brain structure-function relationships by predicting SC from FC [15], [16] or FC from SC [17]–[19]. However, these studies are limited by their focus on unidirectional prediction, neglecting the potential benefits of bi-directional SC-FC translation, which allows inverse mapping of the connectomes.

Motivated by the aforementioned challenges, we propose Structural-Functional Connectivity Generative Adversarial Network (SFC-GAN), a novel framework enabling direct and inverse mapping of individual SC and FC. The key contributions of this work are as follows: (1) To the best of our knowledge, this is the first study to explore bidirectional translation between structural and functional connectomes. We leverage the CycleGAN architecture [20], incorporating convolutional layers to effectively capture the intricate spatial structure of brain connectomes. (2) To maintain the topological integrity of the connectomes, we employ a structure-preserving

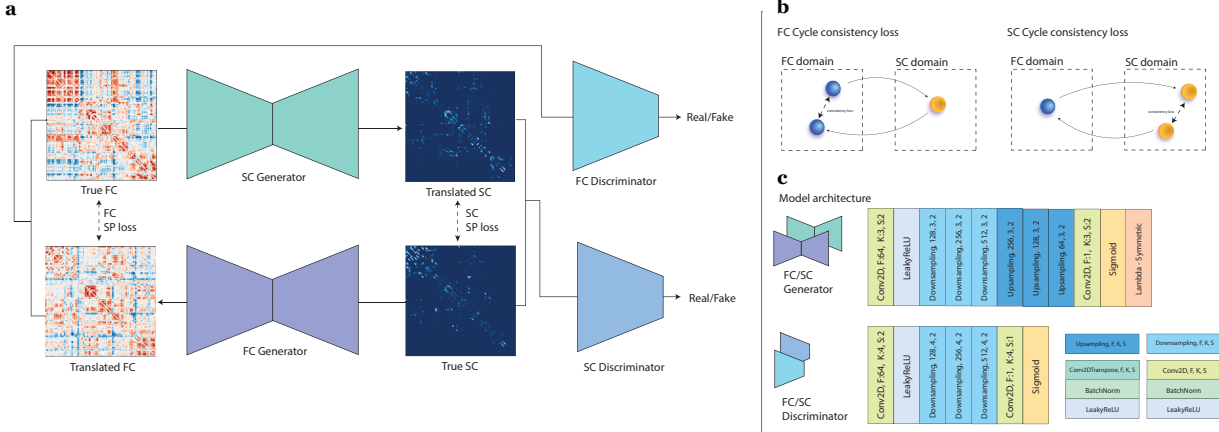


Fig. 1: Overview of SFC-GAN: **a** Training of SFC-GAN, G_{SC} translates FC, x_{fc} to SC \tilde{x}_{sc} , where G_{FC} translates SC, x_{sc} to FC \tilde{x}_{fc} . D_{FC} and D_{SC} aim to discriminate between x_{fc} and \tilde{x}_{fc} , x_{sc} and \tilde{x}_{sc} , respectively. **b** Cycle consistency loss of FC and SC domains. **c** Network architectures of G_{FC} , G_{SC} , D_{FC} , and D_{SC} .

loss inspired by [15], which guides the model in capturing both global and local connectome patterns. Additionally, we design the network architecture to preserve the symmetry inherent in these connectomes. SFC-GAN demonstrates superior performance in translating connectomes, and unveils individual structure-function relationships, making it particularly valuable in scenarios where one of the connectomes is unavailable.

II. METHODS

A. Problem Formulation

We estimate brain FC as an $n \times n$ cross-correlation matrix between fMRI time series and SC as the fiber counts over n brain regions of interest, respectively. Let \mathcal{X}_{FC} and \mathcal{X}_{SC} be a set of FCs and SCs, such that $x_{FC} \in \mathcal{X}_{FC}$ and $x_{SC} \in \mathcal{X}_{SC}$. Given x_{FC} , we aim to translate it to SC \tilde{x}_{SC} , and vice versa from x_{SC} to \tilde{x}_{FC} , while preserving the connectome topology. The ultimate goal is to learn mapping functions θ_{SC} from x_{FC} to \tilde{x}_{SC} , and θ_{FC} from x_{SC} to \tilde{x}_{FC} .

B. SFC-GAN

We introduce SFC-GAN, an extension of the CycleGAN [20], designed to translate between individual FC and SC pairs while preserving connectome topology. The proposed model comprises two generators, G_{SC} and G_{FC} , and two discriminators, D_{SC} and D_{FC} as illustrated in Fig. 1a.

Similar to CycleGAN, we adopt the adversarial loss, with $G_{FC} : X_{SC} \rightarrow \tilde{X}_{FC}$ and $G_{SC} : X_{FC} \rightarrow \tilde{X}_{SC}$, where the objective for G_{FC} is expressed as:

$$\mathcal{L}_{GAN}(G_{FC}, D_{SC}, x_{FC}, \tilde{x}_{SC}) = \mathbb{E}_{x_{SC} \sim p_{SC}} [\log D_{SC}(x_{SC})] + \mathbb{E}_{x_{FC} \sim p_{FC}} [\log(1 - D_{SC}(\tilde{x}_{SC}))] \quad (1)$$

The loss for G_{SC} follows $\mathcal{L}_{GAN}(G_{SC}, D_{FC}, x_{SC}, \tilde{x}_{FC})$, where $\tilde{x}_{FC} = G_{FC}(x_{SC})$ and $\tilde{x}_{SC} = G_{SC}(x_{FC})$. Consistency loss is employed to consistency mappings between FC/SC pairs (Fig. 1b), following:

$$\mathcal{L}_{cyc}(G_{FC}, G_{SC}) = \mathbb{E}_{x_{SC} \sim p_{SC}} [\|\tilde{x}_{SC} - x_{SC}\|_1] + \mathbb{E}_{x_{FC} \sim p_{FC}} [\|\tilde{x}_{FC} - x_{FC}\|_1] \quad (2)$$

To encourage the generators to preserve the connectome structure if the connectome belongs to the target domain, we incorporate the identity loss as in (7).

$$\mathcal{L}_{id}(G_{FC}, G_{SC}) = \mathbb{E}_{x_{FC} \sim p_{FC}} [\|G_{FC}(x_{FC}) - x_{FC}\|_1] + \mathbb{E}_{x_{SC} \sim p_{SC}} [\|G_{SC}(x_{SC}) - x_{SC}\|_1] \quad (3)$$

where the $L1$ norm above encourages that the generators produce identical connectomes given connectomes in the same domain, penalizing deviations. Inspired by [15], we adopt the structure-preserving loss, composed of the mean squared error (MSE) and Pearson correlation coefficient (PCC) loss:

$$\mathcal{L}_{SP}(G_{FC}, G_{SC}) = \mathcal{L}_{PCC}(x_{FC}, \tilde{x}_{SC}) + \mathcal{L}_{PCC}(x_{SC}, \tilde{x}_{FC}) + \mathcal{L}_{MSE}(x_{FC}, \tilde{x}_{FC}) + \mathcal{L}_{MSE}(x_{SC}, \tilde{x}_{SC}) \quad (4)$$

where $\mathcal{L}_{MSE}(\cdot, \cdot)$ ensures element-wise similarity between connectomes, and $\mathcal{L}_{PCC}(\cdot, \cdot)$ measures the correlation between any given pairs of connectomes as defined in (5). Specifically, $\mathcal{L}_{PCC-b}(\cdot, \cdot)$ and $\mathcal{L}_{PCC-r}(\cdot, \cdot)$ measure the correlations across the entire brain and within individual brain regions (each row/column of the connectome), respectively.

$$\mathcal{L}_{PCC}(x, \tilde{x}) = \mathcal{L}_{PCC-b}(x, \tilde{x}) + \mathcal{L}_{PCC-r}(x, \tilde{x}) = \frac{\sum_{i=1}^n \sum_{j=1}^n (x_{i,j} - \bar{x})(\tilde{x}_{i,j} - \bar{\tilde{x}})}{\sqrt{\sum_{i=1}^n \sum_{j=1}^n (x_{i,j} - \bar{x})^2} \sqrt{\sum_{i=1}^n \sum_{j=1}^n (\tilde{x}_{i,j} - \bar{\tilde{x}})^2}} + \sum_{i=1}^n \frac{\sum_{j=1}^n (x_{i,j} - \bar{x})(\tilde{x}_{i,j} - \bar{\tilde{x}})}{\sqrt{\sum_{j=1}^n (x_{i,j} - \bar{x})^2} \sqrt{\sum_{j=1}^n (\tilde{x}_{i,j} - \bar{\tilde{x}})^2}} \quad (5)$$

We follow [12] in designing G_{FC} and G_{SC} architectures to preserve the symmetry structure of the connectomes. Altogether, the generators G_{FC} and G_{SC} and discriminators D_{FC} and D_{SC} are trained in a fashion following:

$$\min_{G_{FC}, G_{SC}} \max_{D_{FC}, D_{SC}} \mathcal{L}_{obj}(G_{FC}, G_{SC}, D_{FC}, D_{SC}) \quad (6)$$

where the objective function of SFC-GAN follows:

$$\begin{aligned}
\mathcal{L}_{obj}(G_{FC}, G_{SC}, D_{FC}, D_{SC}) &= \mathcal{L}_{GAN}(G_{FC}, D_{SC}, x_{FC}, \tilde{x}_{SC}) \\
&+ \mathcal{L}_{GAN}(G_{SC}, D_{FC}, x_{SC}, \tilde{x}_{FC}) \\
&+ \mathcal{L}_{cyc}(G_{FC}, G_{SC}) + \mathcal{L}_{id}(G_{FC}, G_{SC}) \\
&+ \mathcal{L}_{SP}(G_{FC}, G_{SC})
\end{aligned} \tag{7}$$

III. EXPERIMENTAL RESULTS

A. Data acquisition and pre-processing

We conducted experiments using two datasets: the Alzheimer’s Disease Neuroimaging Initiative (ADNI) and the DUMC-MDD dataset, collected at Duke University Medical Center (DUMC). The ADNI dataset included 40 normal controls (CN), 40 individuals with mild cognitive impairment (MCI), and 40 Alzheimer’s disease (AD) patients. The fMRI data from ADNI were processed using the Data Processing Assistant for Resting-State fMRI (DPARSF) following [21], [22]. DMRI data were processed using the Pipeline for Analyzing brain Diffusion imAges (PANDA) software [23] with a standard pipeline and deterministic tractography. The DUMC-MDD dataset consisted of 43 subjects, including 23 CN and 20 major depressive disorder (MDD) participants. Detailed pre-processing procedures for the DUMC-MDD dataset can be found in [24], [25]. For all FC and SC, we employed the

Automated Anatomical Labeling (AAL) atlas to parcellate the brain into 116 regions of interest.

B. Translated connectome evaluation

The performance of the translated connectomes was assessed using several metrics, including Mean Square Error (MSE), Mean Absolute Error (MAE), Structural Similarity Index Measure (SSIM), Pearson correlation, and cosine similarity. Additionally, we examined key graph properties, such as density, characteristic path length (CPL), global efficiency, and modularity, by calculating their Absolute Percentage Difference (APD) relative to the ground truth. We also examine the similarity performance with/without the incorporation of \mathcal{L}_{SP} . A classification study was conducted using a support vector machine (SVM) [26] to determine how well the translated connectomes preserved classification accuracy when compared to the ground truth.

C. Implementation details

The SFC-GAN model was implemented in TensorFlow [27]. The detailed architecture of SFC-GAN is illustrated in Fig. 1c. SFC-GAN was trained for 200 epochs using the Adam optimizer [28]. Both the learning rate and weight decay were set to 0.0001. The model’s performance was evaluated on

TABLE I: Translated FC and SC similarity and graph property evaluation with the incorporation of \mathcal{L}_{SP} .

Loss	Dataset	Data type	Similarity Evaluation					Graph Property APD			
			MSE	MAE	SSIM	Pearson	Cosine	Density	CPL	Efficiency	Modularity
Without \mathcal{L}_{SP}	ADNI	Translated FC	0.0230 ± 0.0046	0.1222 ± 0.0130	32.61 ± 5.41	34.19 ± 8.76	97.62 ± 0.43	10.92 ± 8.05	6.65 ± 4.97	4.69 ± 3.44	75.85 ± 37.30
		Translated SC	0.0050 ± 0.0001	0.0214 ± 0.0011	31.79 ± 2.57	4.03 ± 1.85	8.94 ± 0.02	155.79 ± 9.38	81.35 ± 8.56	70.27 ± 8.39	192.54 ± 5.89
	DUMC-MDD	Translated FC	0.0210 ± 0.0015	0.1141 ± 0.0046	14.76 ± 1.51	34.46 ± 2.05	95.13 ± 0.31	26.35 ± 8.41	5.25 ± 2.23	6.22 ± 2.33	104.11 ± 28.72
		Translated SC	0.0110 ± 0.0001	0.0305 ± 0.0002	37.65 ± 6.84	57.60 ± 0.35	59.20 ± 3.41	74.85 ± 10.97	44.76 ± 4.19	32.68 ± 4.24	109.63 ± 13.89
With \mathcal{L}_{SP}	ADNI	Translated FC	0.0191 ± 0.0055	0.1099 ± 0.0154	37.00 ± 7.18	43.30 ± 7.35	98.03 ± 5.11	8.55 ± 6.89	6.18 ± 4.72	3.89 ± 3.09	72.81 ± 47.73
		Translated SC	0.0001 ± 0.0001	0.0017 ± 0.0012	92.58 ± 6.45	55.63 ± 9.20	56.85 ± 9.01	153.04 ± 9.88	77.25 ± 8.73	68.04 ± 8.47	192.39 ± 5.97
	DUMC-MDD	Translated FC	0.0237 ± 0.0013	0.1224 ± 0.0036	24.45 ± 2.22	41.85 ± 2.06	94.59 ± 2.87	8.49 ± 5.58	3.99 ± 2.02	2.95 ± 1.83	30.45 ± 25.59
		Translated SC	0.0191 ± 0.0055	0.0083 ± 0.0002	81.24 ± 0.67	94.33 ± 2.48	94.49 ± 2.40	72.26 ± 11.53	40.10 ± 4.23	30.22 ± 4.25	112.00 ± 14.73

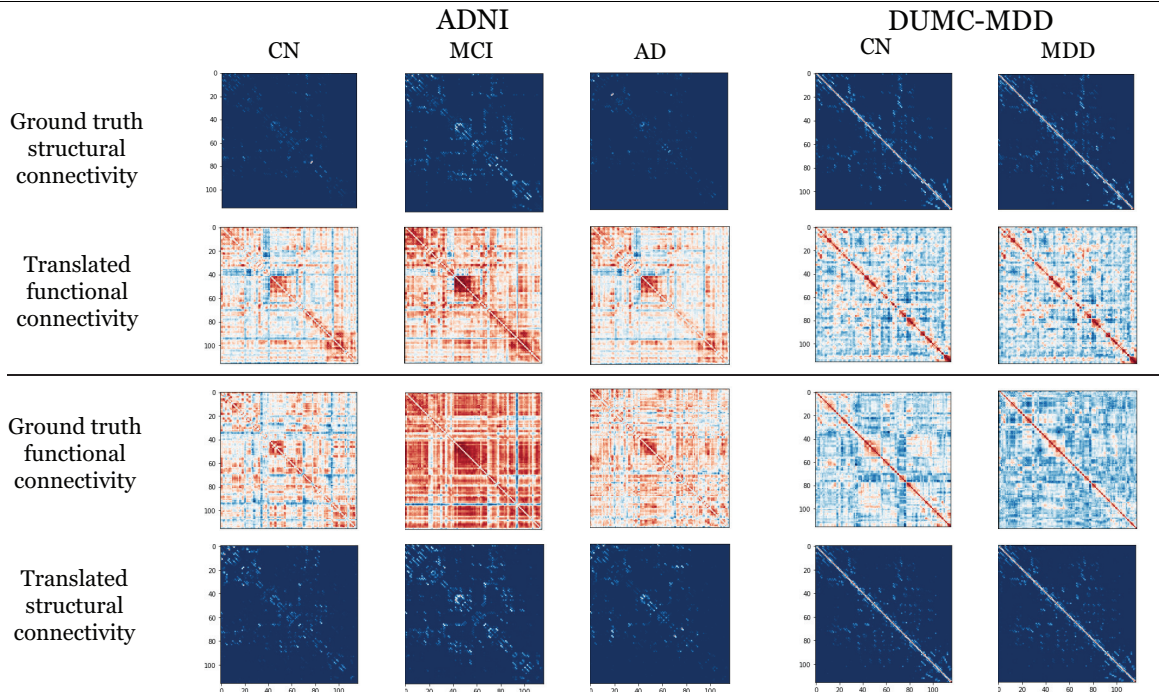


Fig. 2: Matrix reconstruction results on both ADNI and DUMC-MDD datasets using SFC-GAN.

TABLE II: Classification performance on ADNI and DUMC-MDD datasets using original and translated SC and FC.

Classifier	Dataset	Testing data	Accuracy	Precision	Recall	F1-Score	AUC
SVM	ADNI	Real FC	66.67	75.69	66.67	62.38	59.17
		Real SC	41.67	45.83	41.67	41.67	61.11
		Real FC and SC	50.00	27.27	50.00	35.29	57.45
		Translated FC	16.67	11.11	16.67	12.50	52.18
		Translated SC	41.67	27.78	41.67	33.33	57.78
		Translated FC and SC	41.67	25.00	41.67	31.25	83.24
	DUMC-MDD	Real FC	69.23	47.93	69.23	56.64	50.00
		Real SC	53.85	44.06	53.85	48.46	100.00
		Real FC and SC	69.23	47.93	69.23	56.64	72.22
		Translated FC	69.23	47.93	69.23	56.64	50.00
		Translated SC	23.08	7.69	23.08	11.54	62.50
		Translated FC and SC	69.23	47.93	69.23	56.64	72.22

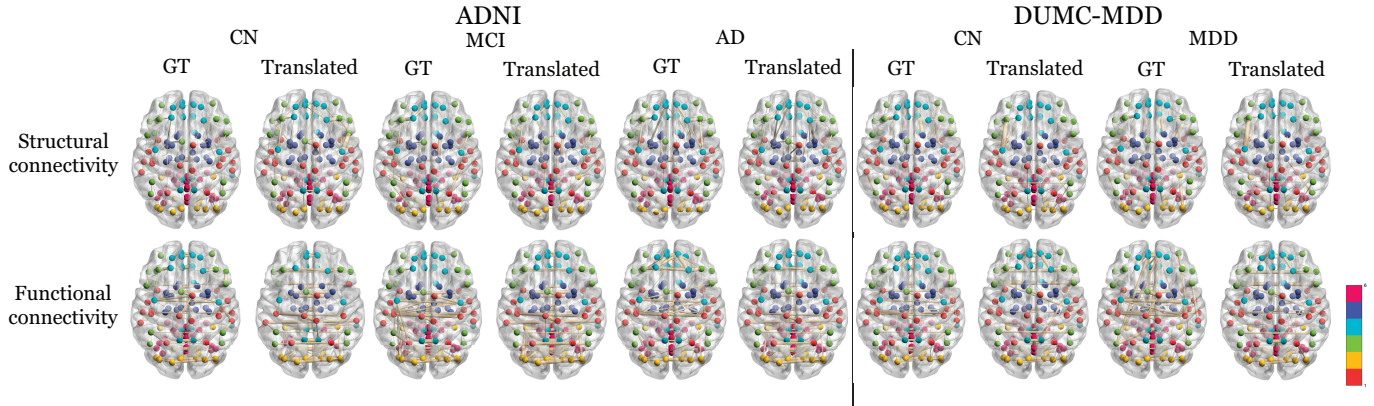


Fig. 3: Reconstruction results on both ADNI and DUMC-MDD datasets with top 5% strongest connectivity in the brain space.

two datasets: the ADNI dataset, with 96 subjects for training and 24 for testing, and the DUMC-MDD dataset, with 30 subjects for training and 13 for testing. For SVM classification, we measured accuracy, precision, recall, F1-score, and Area Under the Curve (AUC) on both real connectomes and those translated from another modality. The data partitioning scheme followed the same approach as used in training the proposed SFC-GAN, where the testing set of SC is translated to FC and vice versa for classification experiments.

Results and discussion: Figures 2 and 3 illustrate the qualitative comparison between the translated connectomes and the ground truth, with matrix reconstruction outcomes and the brain space visualization of the top 5% strongest connections after proportional thresholding for a representative subject. The analysis demonstrates that the translated FC and SC successfully preserve the topological structure of the connectomes, with the visual patterns closely aligning with the ground truth. Furthermore, the top 5% connectivity between the ground truth and the translated connectomes shows a high degree of similarity, indicating that SFC-GAN effectively captures the complex relationships between individual SC and FC, enabling accurate connectomes translation.

Table I presents the similarity metrics and graph property evaluations for the translated connectomes compared to the ground truth. The results demonstrate consistently lower MSE and MAE across both datasets, along with highly comparable graph properties in the translated FC for both testbeds. Notably, the incorporation of the structure-preserving loss, \mathcal{L}_{SP} , enhances performance across all metrics, underscoring its effectiveness in training SFC-GAN to maintain the connectomes topological structure. The translated FC connectomes,

across both the ADNI and DUMC-MDD datasets, exhibit better graph property alignment with the ground truth and higher cosine similarity, although they show lower SSIM and Pearson correlation compared to the translated SC connectomes. This suggests that while the generated FC from SC preserves the overall topological structure, it may not capture the finer details of SC. On the other hand, the translated SC connectomes display consistent performance across both similarity and graph property evaluations, indicating a stronger ability of the model to capture the relationship from FC to SC than from SC to FC. Table II reports the classification performance on the ADNI and DUMC-MDD datasets. The results show that the translated SC and the combined SC and FC connectomes in the ADNI testbed, as well as the translated FC and the combined SC and FC connectomes in the DUMC-MDD testbed, achieve classification performance that is closely aligned with the ground truth. This suggests that the translated connectomes are well-suited for subsequent analyses. However, we observed that the translated FC in the ADNI testbed and the translated SC in the DUMC-MDD testbed exhibited inferior classification performance, indicating areas where further refinement is needed to enhance model performance, offering a powerful approach to understanding and modeling the complex dynamics of brain connectivity.

IV. CONCLUSION

We developed a novel SFC-GAN, incorporating specialized layer and a structure-preserving loss, to enable both direct and inverse mapping between FC and SC while maintaining the topological order and symmetry properties. Our qualitative and quantitative results demonstrate that the model can accurately translate between SC and FC.

REFERENCES

- [1] S.-H. Chu, K. K. Parhi, and C. Lenglet, "Function-specific and enhanced brain structural connectivity mapping via joint modeling of diffusion and functional mri," *Scientific reports*, vol. 8, no. 1, pp. 4741, 2018.
- [2] S. Wein, et al., "Brain connectivity studies on structure-function relationships: A short survey with an emphasis on machine learning," *Computational intelligence and neuroscience*, vol. 2021, no. 1, pp. 5573740, 2021.
- [3] F. Zamani Esfahlani, et al., "Local structure-function relationships in human brain networks across the lifespan," *Nature communications*, vol. 13, no. 1, pp. 2053, 2022.
- [4] P. Skudlarski, et al., "Measuring brain connectivity: diffusion tensor imaging validates resting state temporal correlations," *Neuroimage*, vol. 43, no. 3, pp. 554–561, 2008.
- [5] C.-Y. Wee, et al., "Identification of mci individuals using structural and functional connectivity networks," *Neuroimage*, vol. 59, no. 3, pp. 2045–2056, 2012.
- [6] Y. Li, et al., "Machine learning based on functional and structural connectivity in mild cognitive impairment," *Magnetic Resonance Imaging*, vol. 109, pp. 10–17, 2024.
- [7] Y.-F. Tan, et al., "A unified framework for static and dynamic functional connectivity augmentation for multi-domain brain disorder classification," in *2023 IEEE International Conference on Image Processing (ICIP)*. IEEE, 2023, pp. 635–639.
- [8] Q. Zuo, et al., "Alzheimer's disease prediction via brain structural-functional deep fusing network," *IEEE Transactions on Neural Systems and Rehabilitation Engineering*, vol. 31, pp. 4601–4612, 2023.
- [9] C. Li, et al., "BrainNetGAN: Data augmentation of brain connectivity using generative adversarial network for dementia classification," in *Deep Generative Models, and Data Augmentation, Labelling, and Imperfections*. Springer, 2021, pp. 103–111.
- [10] Q. Yao and H. Lu, "Brain functional connectivity augmentation method for mental disease classification with generative adversarial network," in *PRCV*. Springer, 2019, pp. 444–455.
- [11] B. Barile, et al., "Data augmentation using generative adversarial neural networks on brain structural connectivity in multiple sclerosis," *Comput. Methods and Programs in Biomedicine*, vol. 206, pp. 106113, 2021.
- [12] Y.-F. Tan, et al., "fMRI Functional Connectivity Augmentation Using Convolutional Generative Adversarial Networks for Brain Disorder Classification," in *2024 IEEE International Symposium on Biomedical Imaging (ISBI)*. IEEE, 2024, pp. 1–5.
- [13] Y.-F. Tan, et al., "Brainfc-cgan: A conditional generative adversarial network for brain functional connectivity augmentation and aging synthesis," in *ICASSP 2024-2024 IEEE International Conference on Acoustics, Speech and Signal Processing (ICASSP)*. IEEE, 2024, pp. 1511–1515.
- [14] H. Kong, et al., "Adversarial learning based structural brain-network generative model for analyzing mild cognitive impairment," in *Chinese Conference on Pattern Recognition and Computer Vision (PRCV)*. Springer, 2022, pp. 361–375.
- [15] L. Zhang, et al., "Predicting brain structural network using functional connectivity," *Medical image analysis*, vol. 79, pp. 102463, 2022.
- [16] L. Zhang, L. Wang, and D. Zhu, "Recovering brain structural connectivity from functional connectivity via multi-gcn based generative adversarial network," in *Medical Image Computing and Computer Assisted Intervention–MICCAI 2020: 23rd International Conference, Lima, Peru, October 4–8, 2020, Proceedings, Part VII 23*. Springer, 2020, pp. 53–61.
- [17] J. Neudorf, S. Kress, and R. Borowsky, "Structure can predict function in the human brain: a graph neural network deep learning model of functional connectivity and centrality based on structural connectivity," *Brain Structure and Function*, vol. 227, no. 1, pp. 331–343, 2022.
- [18] Y. Li, G. Mateos, and Z. Zhang, "Learning to model the relationship between brain structural and functional connectomes," *IEEE Transactions on Signal and Information Processing over Networks*, vol. 8, pp. 830–843, 2022.
- [19] Y. Li, et al., "Supervised graph representation learning for modeling the relationship between structural and functional brain connectivity," in *ICASSP 2020-2020 IEEE International Conference on Acoustics, Speech and Signal Processing (ICASSP)*. IEEE, 2020, pp. 9065–9069.
- [20] J.-Y. Zhu, et al., "Unpaired image-to-image translation using cycle-consistent adversarial networks," in *Proceedings of the IEEE international conference on computer vision*, 2017, pp. 2223–2232.
- [21] C.-G. Yan, et al., "Reduced default mode network functional connectivity in patients with recurrent major depressive disorder," *Proc. of the National Academy of Sci.*, vol. 116, no. 18, pp. 9078–9083, 2019.
- [22] C. Yan and Y. Zang, "DPARSF: a matlab toolbox for" pipeline" data analysis of resting-state fMRI," *Frontiers in Syst. Neurosci.*, p. 13, 2010.
- [23] Z. Cui, et al., "Panda: a pipeline toolbox for analyzing brain diffusion images," *Frontiers in human neuroscience*, vol. 7, pp. 42, 2013.
- [24] K. M. Albert, et al., "Brain network functional connectivity and cognitive performance in major depressive disorder," *J. Psychiatr. Res.*, vol. 110, pp. 51–56, 2019.
- [25] R. Wang, et al., "A bayesian approach to examining default mode network functional connectivity and cognitive performance in major depressive disorder," *Psychiatry Res. Neuroimaging*, vol. 301, pp. 111102, 2020.
- [26] C.-C. Chang and C.-J. Lin, "LIBSVM: A library for support vector machines," *ACM Trans. Intell. Syst. Technol.*, vol. 2, no. 3, pp. 1–27, 2011.
- [27] M. Abadi, et al., "Tensorflow: Large-scale machine learning on heterogeneous distributed systems," *arXiv preprint arXiv:1603.04467*, 2016.
- [28] D. P. Kingma and J. Ba, "Adam: A method for stochastic optimization," *arXiv preprint arXiv:1412.6980*, 2014.